International Journal of Occupational Safety and Ergonomics (*JOSE*) 2010, Vol. 16, No. 2, 217–229

Analysis of Steam Formation and Migration in Firefighters' Protective Clothing Using X-Ray Radiography

Corinne Keiser

Empa – Materials Science and Technology, Laboratory for Protection and Physiology, St. Gallen, Switzerland

Peter Wyss

Empa – Materials Science and Technology, Laboratory for Electronics and Metrology, Dübendorf, Switzerland

René M. Rossi

Empa – Materials Science and Technology, Laboratory for Protection and Physiology, St. Gallen, Switzerland

X-ray radiography was used to quantify evaporation and moisture transfer in a multilayer firefighter protective clothing system with defined wetted layers exposed to low thermal radiation. Evaporation was faster and took place at higher temperatures if the moisture was located in the outer layers of the clothing system. Moisture that evaporated in the outer layers of the clothing system was found to move inwards and condense in the inner layers and on the cap of the measurement cell. Results found in this study correlated well with the findings of our former study based on simple temperature distribution measurements to determine moisture transfer in protective clothing layers at low level thermal radiation.

X-ray radiography evaporation steam transfer protective clothing firefighting heat and mass transfer

1. INTRODUCTION

Firefighters usually work in a hot and very moist environment, which leads to a large moisture accumulation in the protective clothing [1, 2, 3, 4]. Moisture trapped in the clothing system strongly affects the heat transfer properties of the clothing. Additionally, this moisture may evaporate, which leads to the risk of steam burns [2, 3, 5]. Steam burns emerge if the firefighter is exposed to an external heat load and moisture within the clothing system starts to evaporate. The emerging hot steam can diffuse to the inside towards the body depending on the permeability of the clothing layers [6] and condenses on the skin [7]. During this condensation process, heat of evaporation is released, which might cause burns.

In a preliminary study, we tried to measure the moisture transfer within protective clothing layers with humidity sensors. The results were

This publication is part of the doctoral dissertation of Corinne Keiser "Steam Burns Moisture Mangement in Firefighter Protective Clothing" (Diss. ETH No. 17406, Zurich, Switzerland), 2007.

Correspondence and requests for offprints should be sent to René M. Rossi, Empa – Materials Science and Technology, Laboratory for Protection and Physiology, Lerchenfeldstrasse 5, CH-9014 St. Gallen, Switzerland. E-mail: <rene.rossi@empa.ch>.

not satisfactory as the temperature and humidity changes were too fast and caused problems in the transient response of the sensors. Furthermore, only relative humidity changes could be measured with humidity sensors. Absolute amounts of moisture and thus condensation within the clothing layers could not be measured.

In a previous study, we analysed the temperature distribution within protective clothing layers including a wet layer [8]. By analysing the temperature courses we found correlations with the evaporation process. In the present work, we measured the total water content and the variations of its distribution with X-ray radiography.

X-ray attenuation technique was already shown to be a valuable tool for analysing of moisture distribution and movement in porous materials. Weder, Bruhwiler and Laib used micro computer tomography to analyse the moisture distribution in multilayer textile assemblies [9]. Roels and Carmeliet analysed moisture flow in porous materials using microfocus X-ray radiography [10]. In the present study, moisture transfer within multilayer protective clothing assemblies at low thermal radiation was analysed using X-ray radiography. The radiography/tomography system was located in a large climatic chamber so that the heat flux of the infrared heater could not damage the X-ray system components.

The aim of the study was to quantify moisture movement within protective clothing layers when exposed to low thermal radiation by analysing the water content of the layers versus time.

2. MATERIALS

The materials used for the experiments are listed in Table 1. They correspond to materials used in state-of-the-art firefighter jackets in combination with aramid underwear and are identical to those used in Keiser and Rossi [8]. The jacket consisted of five layers; a heat resistant outer shell, a water vapour permeable membrane, two layers of a thermal barrier (1 and 2) and a liner.

All samples were washed once at 40 °C according to Standard No. ISO 6330:2000 [13] procedure 5A/40 °C prior to our test measurements to remove residues of finishes. The samples were stored at standard environmental conditions (20 °C, 65%). Therefore, they contained moisture according to their regain of ~5%.

3. METHODS

Figure 1 shows the setup, which is described in more details in Keiser and Rossi [8]. It consisted of an upright standing polyether ether ketone (PEEK) tube positioned below an infrared radiation source. The samples were placed horizontally inside the tube, where they were clamped between two aramid nets. The upper

TABLE 1. Materials Used for the Measurements and Their Mass, Thickness, Water Vapour Resistance (R_{et}) and Thermal Resistance (R_{ct}, Both Measured According to Standard No. EN 31092:1994 [11]).

Part of Assembly	Denomination	Material	Mass (g/m^2)	Thickness [12]	R_{et} (m^2Pa/W)	R_{ct} (m^2K/W)
Underwear	UW	aramid underwear knit	140	1.43	4.46	38.3×10^{-3}
Jacket						
liner	IL	aramid inner liner	115	0.51	3.04	18.2×10^{-3}
thermal barrier 2 layers	TB1 and TB2	aramid nonwoven fabric	50	1.06	2.80	29.7×10^{-3}
membrane	MB	PTFE membrane laminated on aramid	135	1.33	13.30	45.3×10^{-3}
outer layer	OL	aramid	185	0.81	3.56	20.0×10^{-3}

Notes. PTFE—polytetrafluoroethylene.

net was weighed down with a lead ring of 100 g to apply a constant pressure onto the samples to ensure that the samples were lying flat. The distance between the thermal radiation source and the samples was calibrated to get a constant thermal radiation flux of 5 kW/m^2 at the upper surface of the samples. This surface was 4 cm from the upper edge of the tube. This arrangement ensured that moisture evaporating in the clothing layers did not flow sideways and thus minimised boundary effects. A polytetrafluoroethylene (PTFE) lid was placed on the bottom of the measurement cell either 1 cm from the lower surface of the samples or in direct contact (no air gap).

To record the temperature within the garment continuously throughout each measurement, T-type (copper-constantan) thermocouples (Harvard Apparatus, USA) were placed between each layer of the garment (Figure 2).

At the beginning of the measurement, one specific layer, i.e., the underwear (UW) or thermal barrier (TB) 2, was wetted with a defined amount of distilled water (i.e., 0.6, 1 or 1.5 g). These amounts corresponded to typical moisture accumulations measured in similar layers during a previous study [1] where we analysed the mass transport in firefighters' ensembles with a sweat release corresponding to 1 L/h for a human body. The different humidity conditions were denominated accordingly (e.g., UW 0.6 or TB 1.0). UW and TB indicate the layers which were wetted and the additional number indicates the amount of moisture initially supplied. The assembly including the wet layer was placed inside the tube and irradiated with 5 kW/m^2 for 10 min. This radiant heat flux corresponded to a typical hazardous condition encountered by firefighters in a house fire, usually reaching intensities between 1 and 10 kW/m^2 [14, 15]. The duration of exposure was considered as a normal operating time for a firefighter in a fire rescue situation.

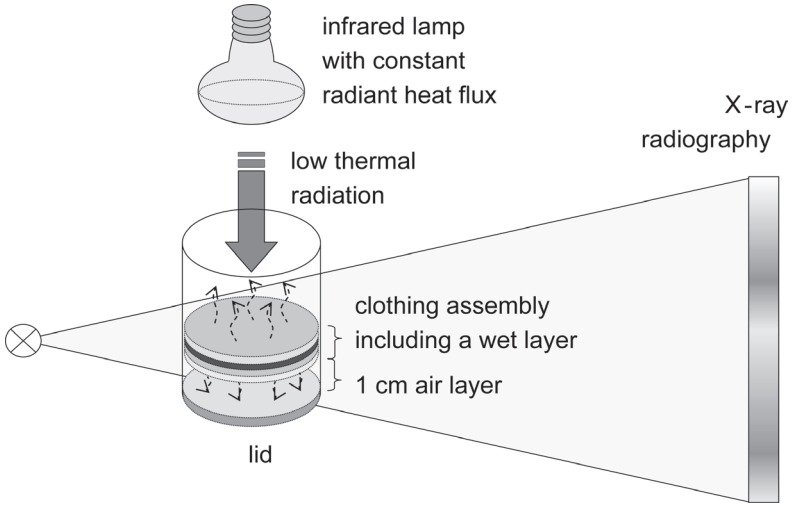

Figure 1. Measurement setup including sample holder, thermal radiation heat source and X-ray source.

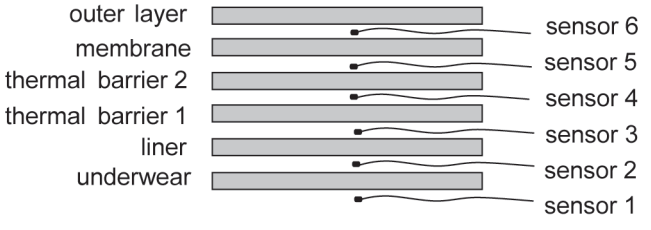

Figure 2. Order of the assembly and the thermocouples between different layers.

3.1. X-ray Radiography

For the X-ray radiography, a directional molybdenum target was used. The window filtering consisted of 0.5 mm beryllium and 0.025 mm silver. This source and the filtering with silver provided a restricted X-ray spectrum ~20 keV thus avoiding beam hardening effects. The X-ray source acceleration energy was 50 keV and the current was set to 0.46 mA. The X-ray spot size was ~100 μm.

The detector was a Hamamatsu 7942 CA-02 flat panel (Hamamatsu Photonics, Japan), operated in 4 × 4 binning mode using single nonaveraged 0.3-s shots. The front face was carbon fibre reinforced plastic. One scan per second was made for 10 min resulting in 600 pictures. The source-to-detector distance was 680 mm and the source-to-sample distance was 180 mm. This resulted in a pixel size referred to sample of 53 μm and a full frame field of view of 30 × 31 mm, based on a full frame of 560 × 592 pixels.

3.2. Evaluation

Figure 3 shows an X-ray radiography taken with the setup of condition TB 1.5 (i.e., 1.5 g water initially located in TB 2). To determine the moisture content within the different layers, quadrangles were defined in the pictures for each layer. Only the middle part on the side without thermocouples was used for the evaluation.

According to Beer's law monochromatic radiation with the intensity I is attenuated over a length d with the linear absorption coefficient μ [16]:

$$\ln\left(\frac{I}{I_0}\right) = -\mu d, \tag{1}$$

where I_0—incident intensity, I—intensity of attenuated X-ray, μ—attenuation coefficient, d—length of X-ray path through sample.

From this equation, the moisture content within each single clothing layer can be derived [10]:

$$M_w = -\frac{\rho_w}{\mu_w d}\ln\left(\frac{I_{wet}}{I_{dry}}\right), \tag{2}$$

where M_w—moisture content of specific layer (kg/m^3), ρ_w—density of liquid water (kg/m^3), μ_w—attenuation coefficient of water, d—irradiated length of sample, I_{wet}—intensity measured for wet sample, I_{dry}—intensity measured for dry sample.

The specific absorption coefficient of each layer had to be determined experimentally as the thickness of the layers and thus the local moisture content within the layers was different for every single layer. Therefore, a calibration for each single layer and different moisture content was performed. To calibrate the moisture measurement we supplied each of the single layers with different amounts of water (0.3, 0.6, 0.9, 1.2 and 1.5 g). Then, X-ray radiographs of each layer with each of the five different amounts of water were taken separately without thermal radiation. Figure 4 shows the calibration curves for UW and TB 2.

Each single layer was calibrated according to its specific calibration curve and the constant C was determined from the linear regression curve:

$$C = \frac{\rho_w}{\mu_w d}. \tag{3}$$

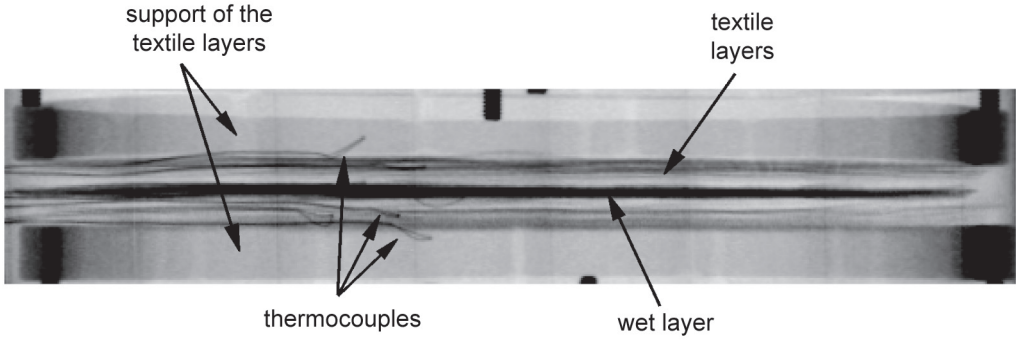

Figure 3. X-ray radiography of condition TB (thermal barrier) 1.5.

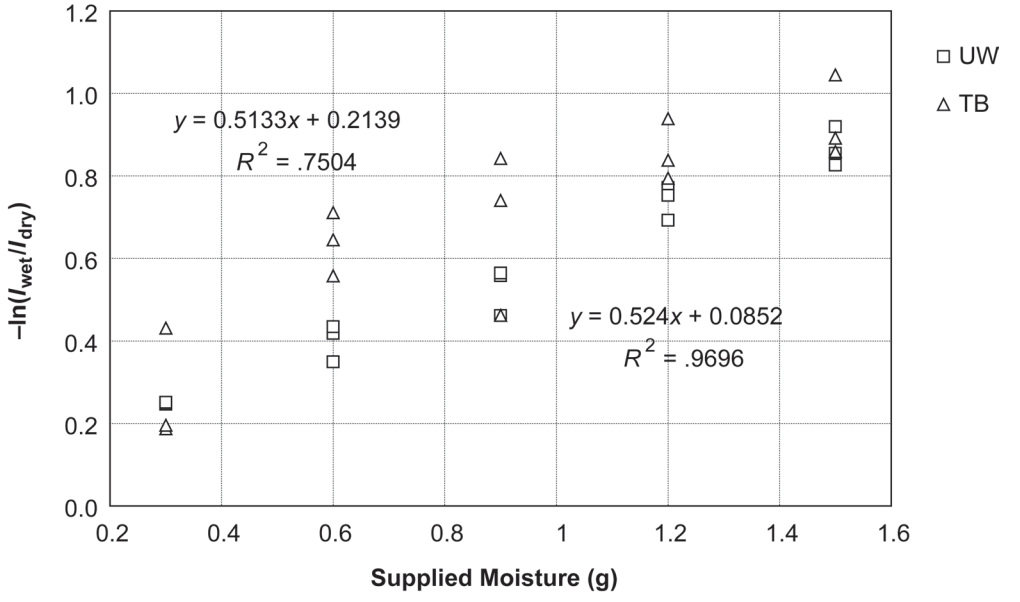

Figure 4. Moisture calibration curves presenting $-\ln(I_{wet}/I_{dry})$ as a function of supplied moisture content of UW (underwear) and TB (thermal barrier). *Notes.* I_{wet}—intensity measured for wet sample, I_{dry}—intensity measured for dry sample.

After this calibration, the curves still showed a certain vertical shift. Therefore, the initial moisture content of the different (dry) layers was set arbitrarily to zero. Negative values in the inner layers at the end of the measurement hence implied that water was initially present in those layers.

4. RESULTS

The amount of water supplied was consistent with the amount measured with the X-ray radiography. For 0.6 g of supplied moisture, the initial moisture content measured in the underwear (UW 0.6) was 0.59 ± 0.03 g and in the thermal barrier (TB 0.6) 0.67 ± 0.09 g. However, there was a linear shift of moisture measured for higher moisture content: the higher the initial moisture content, the bigger the difference between the supplied and the measured moisture content. For UW 1.0 only 0.92 ± 0.03 g moisture was detected, for TB 1.0 the detected amount was 0.93 ± 0.04 g, for UW 1.5 we obtained 1.22 ± 0.08 g and for TB 1.5 only 1.20 ± 0.03 g.

Figure 5 shows the results of the X-ray radiography measurements with 1 g of water initially located in the underwear (UW 1.0) or in the thermal barrier 2 (TB 1.0). The decrease in the moisture in the initial wet layer is visible for both conditions (a) in UW and (b) in TB 2. The innermost two layers of the system (underwear UW and liner IL) showed a moisture increase during the evaporation phase when water was initially in TB 2. When water was initially in the underwear, the inner layer of the jacket (IL) showed an initial increase in moisture content. TB 1 (without initial moisture) reached negative moisture content at the end of the measurement, which implies that moisture must have been initially present in this layer. The mean standard deviations of the different conditions ranged up to 0.07 g.

The outer layer of the combination showed an initial decrease in moisture but an increase at the end.

4.1. Evaporation

Figure 6 shows the decrease in the moisture content within the initially wet layers. We arbitrarily defined the start of evaporation as the time when the decrease in the moisture content reached 0.05 g in 3 s. For the wet underwear, the moisture content stayed constant in the beginning for ~30–60 s. However, these values varied greatly with standard deviations up to 34 s. For the wet TB, the moisture content decreased right

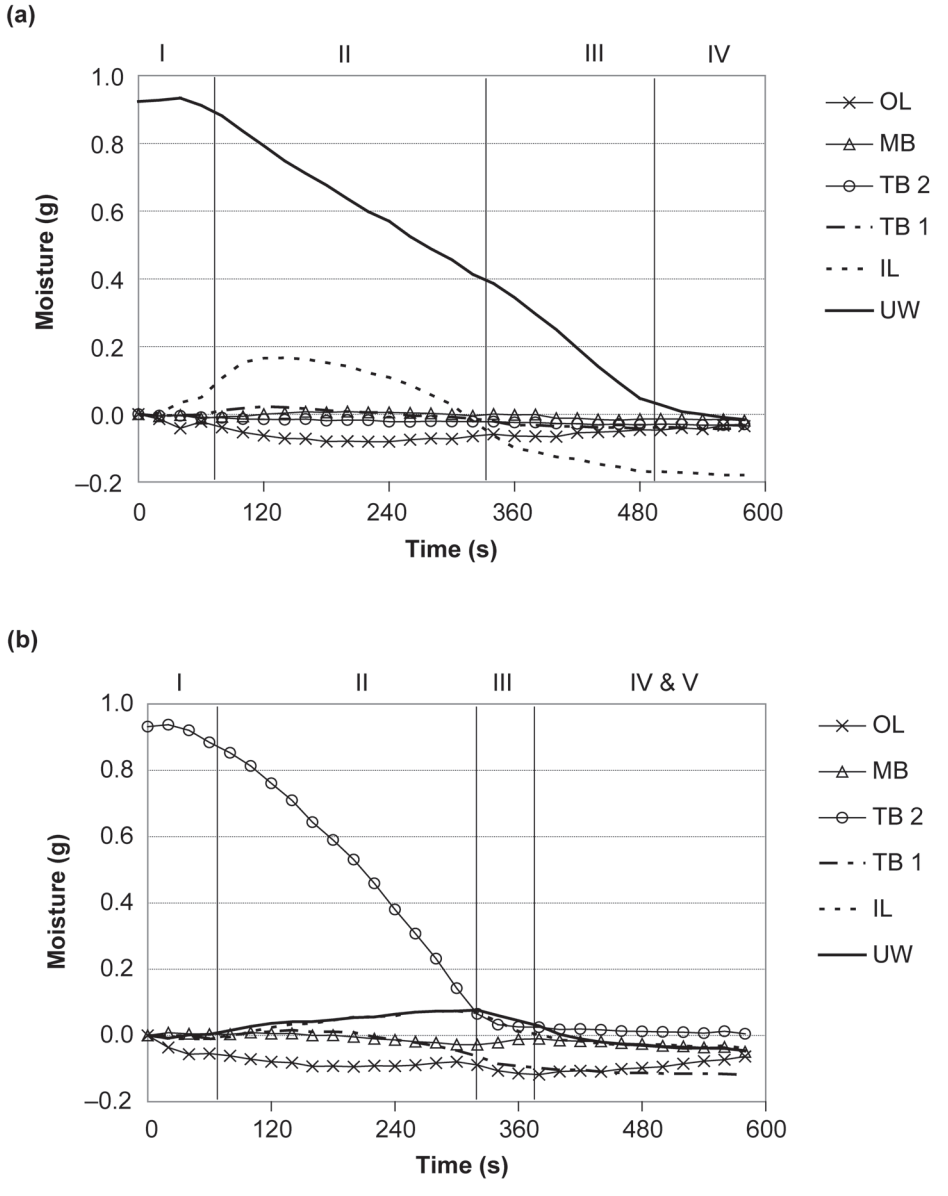

Figure 5. Moisture content in different layers measured with X-ray radiography for 1 g of moisture initially located in (a) underwear (UW 1.0) and (b) thermal barrier 2 (TB 1.0). *Notes.* OL—outer layer, MB—membrane, IL—liner.

from the beginning for the two conditions with higher moisture content (TB 1.0 and TB 1.5). For TB 0.6 the evaporation started after 33 ± 17 s. In the measurements without air gap, evaporation started with a delay of 103 ± 31 s for UW conditions and of 33 ± 21 s for TB conditions.

The moisture decrease in the conditions with wet UW was linear with time and the evaporation rate was very similar for all three conditions with an air gap. In the conditions with wet TB, the decrease in moisture was not linear throughout the evaporation process but the evaporation rate was again similar for all conditions. The evaporation was slower for wet UW than for wet TB. The air gap had no influence on the evaporation rate with wet TB. However, with wet UW, the evaporation was slower with an air gap.

The mean evaporation rate was calculated for moisture content of 0.5–0.2 g, and alternatively between 0.8 and 0.5 g for UW 1.0 without an air gap and UW 1.5 as the moisture content of 0.2 g was not reached at the end of the measurement for these two conditions. Table 2 shows the results. The evaporation rates with wet UW were

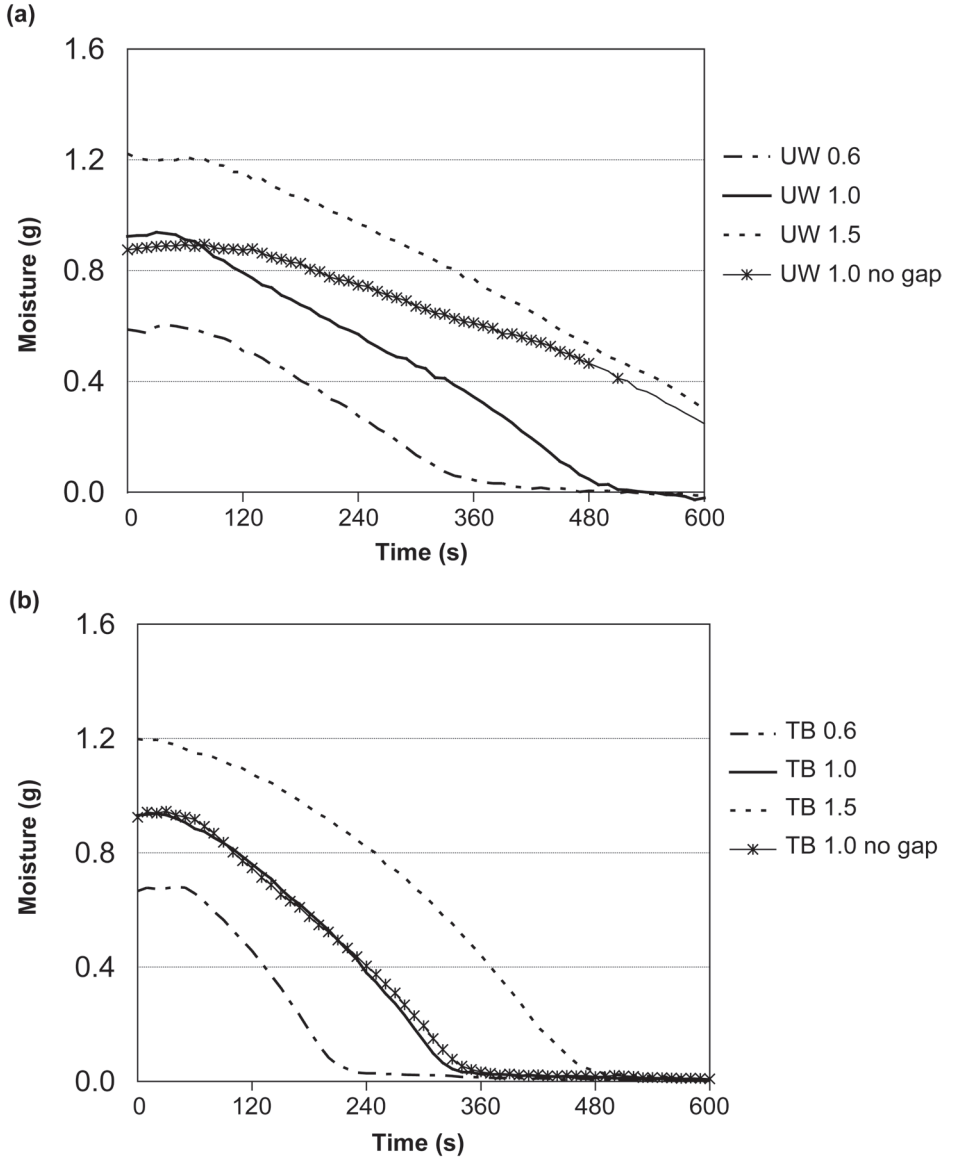

Figure 6. Change in moisture content with time in the initially wet layer for (a) UW (underwear) and (b) TB (thermal barrier) conditions.

smaller than with wet TB. The evaporation rate in UW without an air gap was about half of the evaporation rate with an air gap. When UW was lying directly on the lid, the evaporation could only take place towards the outer side of the sample. To take into account this smaller evaporating surface, we normalised it by the evaporating surface of 77 cm^2 and respectively of 38 cm^2 for condition UW 1.0 without an air gap (Table 2).

TABLE 2. Mean Evaporation Rates for Different Conditions; Absolute and per Evaporating Surface

Condition	Evaporation Rate (*SD*) (g/s)	Evaporation Rate per Evaporating Surface Area (*SD*) (g/m^2s)
UW 0.6	$2.1\ (0.14) \cdot 10^{-3}$	0.27 (0.02)
UW 1.0	$2.1\ (0.01) \cdot 10^{-3}$	0.27 (0.01)
UW 1.5	$1.9\ (0.03) \cdot 10^{-3}$	0.24 (0.01)
UW 1.0 without gap	$1.2\ (0.11) \cdot 10^{-3}$	0.30 (0.03)
TB 0.6	$4.4\ (0.98) \cdot 10^{-3}$	0.58 (0.13)
TB 1.0	$3.8\ (0.41) \cdot 10^{-3}$	0.49 (0.05)
TB 1.5	$4.0\ (0.20) \cdot 10^{-3}$	0.52 (0.03)
TB 1.0 without gap	$3.3\ (0.29) \cdot 10^{-3}$	0.43 (0.04)

4.2. Moisture Accumulation in the Inner Layers

Figure 7a shows the moisture accumulation in UW for the initially wet TB. During evaporation UW absorbed up to 0.18 g of water with standard deviations between 0.01 and 0.07 g. Moisture continuously increased until it reached a maximum and then decreased again. The higher the initial moisture content of TB was, the later the maximal moisture content of UW was reached. Figure 7 b shows the moisture accumulation in the liner for the measurements with wet UW. The initial moisture increase was much larger than with wet TB. Maximal moisture content of 0.2 ± 0.7 g was reached at about the same time, independently of the amount of the initial moisture content. However, the maximal moisture content absorbed by the liner depended

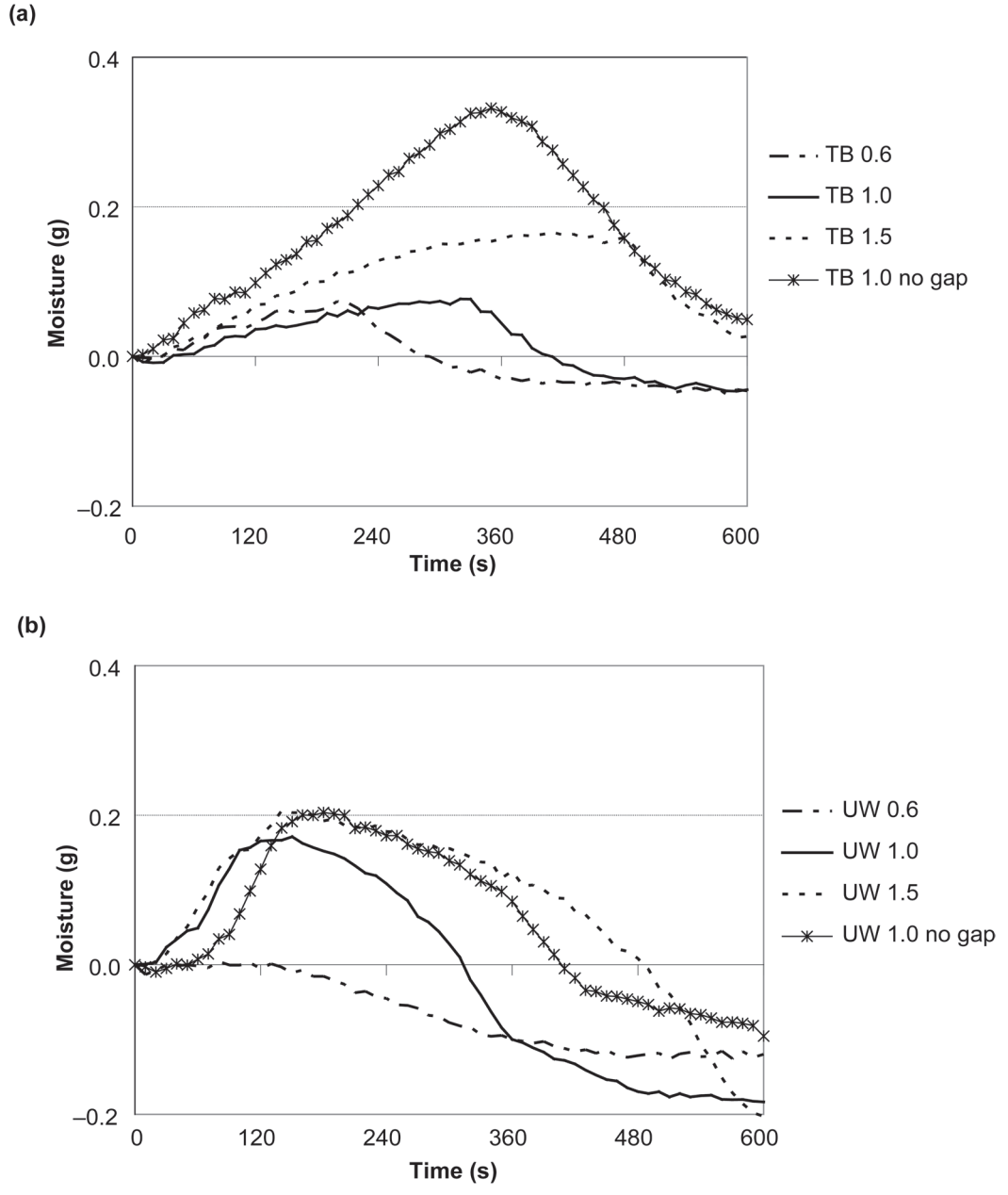

Figure 7. Changes in moisture content with time in (a) the underwear of TB (thermal barrier) conditions and (b) the liner of UW (underwear) conditions for different initial moisture content and measurements with and without an air gap.

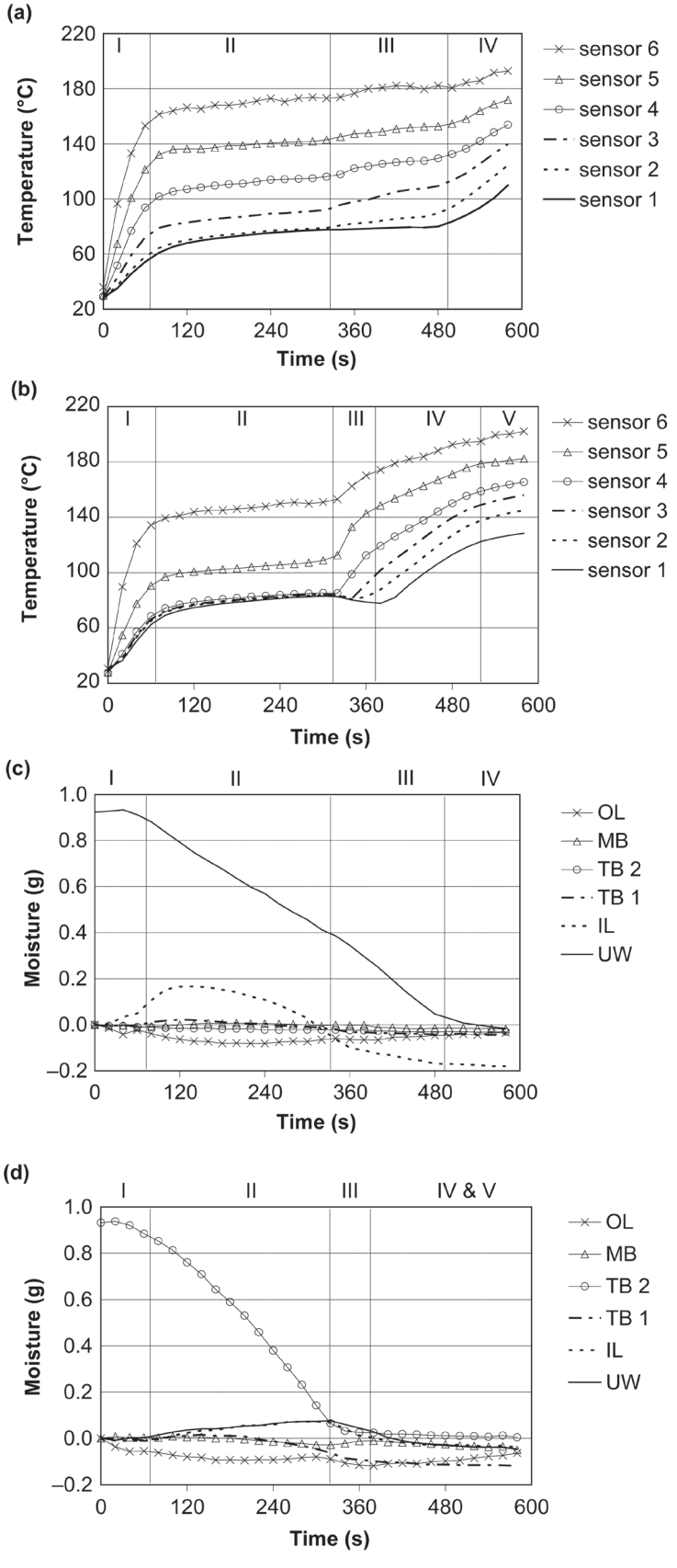

Figure 8. Comparison between temperatures within clothing layers [8] and moisture content; (a) temperatures of UW (underwear) 1.0, (b) temperatures of TB (thermal barrier) 1.0, (c) moisture content of UW 1.0 and (d) moisture content of TB 1.0.

on the initial amount of moisture in the systems (0.01 ± 0.01 g for UW 0.6, 0.18 ± 0.05 g for UW 1.0 and 0.22 ± 0.06 g for UW 1.5). This dependency was not found with initial wet TB. The maximal moisture content in UW for TB (wet) condition was much larger (3.5 ± 0.5 times) in the measurements without than with an air gap.

It is interesting to note that the moisture content of the liner was always negative at the end of the measurements. A similar observation was made in TB 1 when TB 2 was wet, showing that some liquid transport must have taken place when assembling the layers before the beginning of the measurement.

No significant moisture increase in the other layers was observed. The outer layer even dried out during the measurement when heating up.

We found a very high correlation between the time necessary to reach the maximal moisture content in the inner layers (i.e., UW and liner) and the time at which evaporation stopped in the initially wetted layer (R^2 = .991 for UW and R^2 = .995 for the liner with initially wet TB), as both occurred at about the same time. The end of evaporation was defined by the time when the decrease in the moisture content in the initially wet layer was lower than 0.05 g in 3 s. With wet UW, it was not possible to make this correlation due to missing evaporation end points of UW 1.0 and UW 1.5. However, maximal moisture content was reached for all conditions at about the same time (127–167 ± 29 s) except for UW 0.6 where the maximal moisture content was reached after 47 ± 34 s. This was more than 300 s earlier than evaporation stopped.

4.3. Comparison Between X-Ray Radiography and Temperature Measurements

Figure 8 shows the temperature curves of the sensors placed between the single layers for (a) conditions UW 1.0 and (b) TB 1.0 as well as the moisture content in the different layers for the same conditions (c) UW 1.0 and (d) TB 1.0. A comparison of the temperatures within the clothing layers and the moisture content shows that evaporation ended at the same time as the temperature equilibrium, i.e., at the end of phase III for UW conditions and at the end of phase II for TB conditions. At the end of phase II of UW conditions the slight temperature rise in the liner coincides with the decrease in the evaporation rate in the liner.

The temperature drop in the inner layers (i.e., UW and liner) at the end of phase II of condition TB 1.0 confirms the findings that moisture has accumulated in those layers, and started evaporating after the end of evaporation of the initially wet TB (Figure 8d).

5. DISCUSSION

The analysis of the moisture content and distribution of the different textile layers with X-ray radiography was not trivial for all layers, especially the upper ones. The horizontal level of the X-ray source was aligned with the lower surface of the sample. Thus, some geometrical shifts are assumed to have appeared at the upper surface. Furthermore, the fibres of the upper support stretched during heat exposure and thus slightly changed the geometry of the upper layers. These shifts of the samples were considered in the evaluation process but probably not all geometric corrections could be fully considered, which resulted in a certain measurement spread.

The measured initial moisture content was lower than the supplied moisture especially at the higher initial moisture content. We suppose that moisture started to wick to the neighbouring layers as soon as the assemblies were put together. Therefore, moisture was also present in the neighbouring layers of the wet layer at the beginning of the X-ray radiography measurement. However, it has been shown that wicking can only occur when a certain threshold value of moisture content in the wet layer is exceeded [17, 18, 19]. Thus, with UW 0.6 (i.e., 0.6 g of water initially located in UW) this threshold value was probably not reached and, therefore, no moisture wicked to the liner.

Evaporation in wet TB started earlier than in wet UW, which can be explained by the temperature gradient with obviously higher temperatures in TB than in UW [8]. Therefore,

evaporation started at a high rate right from the beginning with wet TB while a delay of the start of evaporation could be seen with wet UW. The evaporation rates did not depend on the initial amount of moisture, but on its location, as the evaporation was slower in wet UW than in wet TB. The presence of an air gap between UW and the lower lid of the sample holder had no effect on the evaporation rate in wet TB. However, with wet UW, the evaporation rate was lower without an air gap. In this condition, UW was lying directly on the cap of the measurement cell. Thus, moisture could only evaporate in one direction. The evaporation surface was half of the evaporation surface of the conditions with an air gap and accordingly, the evaporation rate was approximately halved.

During the course of the heat exposure, moisture could be measured in the inner layers (i.e., UW and liner). In the conditions with initially wet TB, moisture accumulated in the liner and UW continuously during evaporation. Only when all moisture had evaporated from TB, did the moisture content of the inner layers start to decrease. Only little moisture was measured in the initially dry TB 1. This shows that the migration of moisture from wet TB 2 to the inner layers (i.e., UW and liner) did not most probably occur by liquid diffusion (wicking), but by evaporation and recondensation in the inner layers. Condensed water could also be found on the cap of the measurement cell during evaporation.

With wet UW, moisture probably started to wick to the liner as soon as the assembly was piled up. Accordingly, some moisture was already present in the inner liner when the measurement started. However, the moisture content in the liner strongly increased with rising temperature. The wicking process seemed to accelerate with increasing temperature. After 147 ± 29 s the wicking stopped and moisture started to evaporate from the liner. This maximal moisture content was reached in all layers at about the same time. One can suppose that wicking (transfer of liquid moisture) only took place until the initially wet layer reached a lower humidity threshold after which the concentration of water was too low to get a transfer between the layers.

The results of the X-ray radiography measurements agreed well with the findings of the temperature measurements of our previous study [8]. The duration of evaporation was very similar with both measurement methods. The start of moisture evaporation coincided with a plateau in temperature. During the largest part of the evaporation phase, the measured temperatures remained nearly constant and the dry heat flux transferred was thus in steady-state. However, an additional, moisture-assisted heat transfer also took place as steam flowed to the inside and recondensed on the lid. In the previous study, we supposed that moisture must have accumulated in the inner layers with initially wet TB. X-ray radiography confirmed these findings. With wet TB, the maximal amounts of moisture accumulated in UW and the liner reached 0.17 ± 0.09 g. For measurements without an air gap, this accumulation even reached 0.34 ± 0.01 g. Condensed moisture was also found on the cap of the measurement cell at the end of the measurement. The temperature measurements showed that the moisture in the innermost two layers caused a temperature drop in the sensors next to these layers (sensors 1–3 according to Figure 8) at the end of the evaporation phase. The quantification of this moisture-assisted heat flux was not possible as no temperature increase was registered by sensor 1 during the moisture condensation. This was probably because most moisture directly condensed on the lid and the heat released must have been dissipated through the lid. To confirm this hypothesis, the lid should be replaced with a calorimeter or a temperature sensing surface in a further study.

6. CONCLUSIONS

We showed in this study that X-ray radiography is a very valuable tool to study quantitatively the distribution of moisture and the evaporation processes within clothing layers. We showed that when a wet outer clothing layer (in our case TB) is exposed to thermal radiation, moisture flowed to the inner layers (i.e., UW and liner) of the

protective clothing. This moisture accumulation was due to evaporated steam in the outer layer that recondensed in the inner layers. Liquid moisture wicking to the inner layers could most probably be excluded as the moisture content of the layer between the initially wet layer and the liner was low.

These results confirm the findings of a previous study that the evaporation rate per surface area was independent of the initial amount of moisture supplied to the clothing assembly, but depended on the localisation of the moisture. Moisture evaporated faster from the outer layers of the assembly than from the inner ones.

Moisture is known to influence the heat transfer through clothing assemblies by changing their thermal properties (thermal conductivity and heat capacity). This study suggests that an additional (moisture-assisted) heat flux takes place by evaporation of moisture in the outer layers and recondensation near the body. The intensity and duration of this additional heat flux depends on the evaporation rate and the amount of moisture stored in the layers. In light of these results, it is suggested that moisture accumulation should be avoided in outer layers of heat protective clothing assemblies.

REFERENCES

1. Keiser C, Becker C, Rossi RM. Moisture transport and absorption in multilayer protective clothing fabrics. Text Res J. 2008:78(7):604–13.
2. Mäkinen H, Smolander J, Vuorinen H. Simulation of the effect of moisture content in underwear and on the skin surface on steam burns of fire fighters. In: Mansdorf SZ, Sager R, Nielsen AP, editors. Performance of protective clothing (ASTM STP 989). West Conshohocken, PA, USA: American Society for Testing and Materials (ASTM); 1988. p. 415–21.
3. Rossi R, Weder M. Untersuchung des Wärme- und Feuchtetransfers bei mehrschichtigen Schutzkleidungen [Analysis of heat and mass transfer in multilayer protective clothing]. In: 5. Dresdner Textiltagung. Dresden, Germany: Institut für Textil- und Bekleidungstechnik (ITB) of TU Dresden; 2000.
4. Schopper-Jochum S, Schubert W, Hocke M. Vergleichende Bewertung des Trageverhaltens von Feuerwehreinsatzjacken (Phase 1) [Comparative assessment of the wearing behaviour of firefighters' protective clothing (Phase 1)]. Arbeitsmedizin, Sozialmedizin und Umweltmedizin. 1997:32(4).
5. Prasad K, Twilley W, Lawson JR. Thermal performance of fire fighters protective clothing. 1. Numerical study of heat and water vapour transfer. Gaithersburg, MD, USA: National Institute of Standards and Technology, Fire Research Division; 2002.
6. Rossi RM, Indelicato E, Bolli W. Hot steam transfer through heat protective clothing layers. International Journal of Occupational Safety and Ergonomics (JOSE). 2004;10(3):239–45.
7. Chitrphiromsri P, Kuznetsov A. Modeling heat and moisture transport in firefighter protective clothing during flash fire exposure. Int J Heat Mass Transf. 2005; 41(3):206–15.
8. Keiser C, Rossi RM.Temperature analysis for the prediction of steam formation and transfer in multilayer thermal protective clothing at low level thermal radiation. Text Res J. 2008;78(11):1025–35.
9. Weder M, Bruhwiler PA, Laib A. X-ray tomography measurements of the moisture distribution in multilayered clothing systems. Text Res J. 2006;76(1):18–26.
10. Roels S, Carmeliet J. Analysis of moisture flow in porous materials using microfocus X-ray radiography. Int J Heat Mass Transf. 2006;49(25–26):4762–72.
11. European Committee for Standardization (CEN). Textiles. Determination of physiological properties. Measurement of thermal and water-vapour resistance under steady-state conditions (sweating guarded-hotplate test). (Standard No. EN 31092:1994). Brussels, Belgium: CEN; 1994.
12. Rossi RM, Zimmerli T. Influence of humidity on the radiant, convective and contact heat transmission through protective clothing materials. In: Johnson JS, Mansdorf, SZ, editors. Performance

of protective clothing (ASTM STP 1237). West Conshohocken, PA, USA: American Society for Testing and Materials (ASTM); 1996. p. 269–80.

13. International Organization for Standardization (ISO). Textiles—domestic washing and drying procedures for textile testing (Standard No. ISO 6330:2000). Geneva, Switzerland: ISO; 2000.
14. Hoschke BN. Standards and specifications for firefighters clothing. Fire Safety Journal. 1981;4(2):125–37.
15. Rossi R. Fire fighting and its influence on the body. Ergonomics. 2003;46(10):1017–33.
16. Krawiz AD. Introduction to diffraction in materials science and engineering. New York, NY, USA: Wiley; 2001.
17. Adler MM, Walsh WK. Mechanisms of transient moisture transport between fabrics. Text Res J. 1984;54(5):334–43.
18. Kissa E. Wetting and wicking. Text Res J. 1996;66(10):660–8.
19. Spencer-Smith JL. The physical basis of clothing comfort, part 4: the passage of heat and water through damp clothing assemblies. Clothing Research Journal. 1977;5(3):116–28.

Symbols

Roman alphabet

C	calibration constant
d	length of the X-ray path through the sample
I_0	incident intensity of the X-ray
I	intensity of the attenuated X-ray
M	moisture content of the layer (kg/m^3)

Greek alphabet

μ	attenuation coefficient
ρ	density

Subscripts

dry	dry sample
w	water
wet	wet sample